FRACTURE MECHANICS ANALYSIS OF THE INFLUENCE OF MACHINING MARKS ON THE LCF LIFE OF THE NICKEL-BASE ALLOY IN 718

G.W. König*

It is well known from failure analysis that inadvertently produced machining or handling marks may result in a dramatic decrease in the fatigue life of turbine engine components. In order to assess the effect of these marks on the fatigue life of the wrought nickel-base alloy IN 718, LCF tests were performed on round smooth specimens under strain controlled loading conditions. Most of the specimens were provided with a circumferential machining groove in the midst of the gauge length. It was found that due to the machining grooves the fatigue life was reduced by a factor of 10 or more. The tests were evaluated with respect to the

- life reduction in relation to the groove depth (20 to 150 microns), loading condition (corresponding to the strain range at critical sites of engine disks), temperature (400 and 600°C) and defect shape
- crack initiation and propagation life
- comparison between the microscopic (striation spacing) and macroscopic crack propagation rate as well as the fracture mechanics predicted crack propagation rate
- influence of shot-peening on the severity of machining grooves as life reducing defects.

With a case study of a turbine disc with a groove in the bore it is demonstrated that the results can be used to estimate the fatigue life of defective engineering components.

1. INTRODUCTION

The useful life of most turbine engine discs is limited by its low cycle fatigue properties. The specific difficulties in the design of discs is due to two basic requirements: A very high safety standard and high operating stresses in critical areas which are necessary to obtain a good engine efficiency. The development of disc materials in the past has been successful in increasing the static strength and the crack initiation life.

* MTU Motoren- und Turbinen-Union, Munich, Germany

Unfortunately, the improvement of the crack initiation behaviour was not accompanied by a similiar improvement of the crack propagation properties [1].
The consequence is that the utilisation of the higher strength potential of new disk materials leads to a strong defect sensivity of fatigue life with respect to defects. Typical defects that were found to decrease the LCF life of high strength nickel-base alloys are nonmetallic inclusions [2/3/4/5] as well as surface inhomogeneities such as for example machining marks [6] or etching grooves.

The conventional way to take into account the scatter in fatigue life caused by defects is to limit the usable life to a certain fraction of the defect-free life by applying a safetyfactor. The disadvantage of this approach is that safetyfactors which are based on the experience of the past may become unsafe when loading conditions or materials are changed. An alternative approach [7] which overcomes this disadvantage is to abandon defect-free testing by tests with specimens and components containing defects of definite size and shape. From these data the effect of the worst defect that is suspected to occur at a critical site of a component can be estimated. Examples for this approach were investigations on nickel-base alloys deliberately doped with ceramic inclusions [4/5] or surface defects produced by electric discharge machining on round bar nickel-base specimens [6]

It was tried to describe the influence of the size of nonmetallic inclusions on the LCF life by fracture mechanics methods [3/4/5]. The analysis is based on the assumption that an inclusion behaves similarly to a fatigue crack of the same size and shape, i.e. that the crack initiation life is small compared with the crack propagation life. Under these circumstances the fatigue life can be estimated by the fracture mechanics crack propagation life. The now available results [5] show that this is true for quite a variety of different inclusion geometries and loading conditions in the LCF life range.

This paper applies a similar fracture mechanics treatment that was successfully used for inclusions to surface defects produced by machining on specimens of the nickel-base alloy IN 718. The aim was to describe the crack propagation life in relation to parameters such as defect size and shape, loading conditions (strain amplitude, mean stress), temperature as well as shot peening treatment. In order to demonstrate the applicability of the results to engine components, a case study of a groove in a turbine disc bore is included.

2. EXPERIMENTAL PROCEDURE

The tests were performed with cylindrical round bar specimens of 9mm diameter under strain controlled loading (strain rate: 3.10^{-3}/second) in the temperature range of 400 to 600°C at a strain ratio R = minimum strain/maximum strain = 0. The surface treatment of the smooth specimens was machining, longitudinal grinding and finally longitudinal polishing. Most of the specimens were provided with a circumferential machining groove in the midst of the gauge length (Fig. 1). The groove depth is in the range of 10 to 150 microns and was determined individually for each specimen from a scanning electron microscope (SEM) micrograph of the fracture surface after testing (Fig. 1a and b). Alternatively the groove depth was determined in some cases by SEM on the surface of the complete specimen before testing (Fig. 1a).

The material used is the wrought nickel-base superalloy IN 718 which is currently used for aero engine disks. A representative micrograph of the microstructure is shown in Fig. 3 . Part of the specimens was shot peened using following parameters: the peening intensity was 0,16 to 0,20 almen, the shot material S 110, the peening angle 90 degrees and the coverage 125 percent. The shot peening treatment of the grooved specimens results in a substantial smoothening of the groove as demonstrated in Fig. 1b. However, at higher magnification it becomes evident that the former groove is not completely removed but continues as a material separation under the surface (Fig. 1b). With some of the specimens the shot peening was performed prior to the machining of the groove.

3. FRACTURE MECHANICS ANALYSIS

According to a fracture mechanics analysis described by Dowling [8] the stress intensity range ΔK of a crack starting from a notch can be divided in two regimes:

For a small crack of depth $a^* < c/(1{,}25\ K_t^2-1)$, where c is the notch depth and K_t the stress concentration factor of the notch, ΔK is derived from the notch root stress $\Delta\sigma_{root}$:

$$\Delta K = 1{,}12\,\Delta\sigma_{root}\sqrt{\pi a^*} \qquad (1)$$

For a large crack, i.e. $a^* > c/(1{,}25\ K_t^2-1)$, ΔK is derived from the nominal stress remote from the notch $\Delta\sigma$

$$K = \Delta\sigma\sqrt{(a^* + c)} \qquad (2)$$

K_t for a semicircular notch is about 3. From SEM evidence (Fig. 1) it was concluded that $K_t \approx 3$ holds for the circumferential grooves, i.e. equation (2) can be applied for $a^* > c/8$. Since the largest part of the fatigue crack depth is in the range $a^* > c/8$ the fracture mechanics prediction was based on equation (2).

The loading which was applied to the specimens is in the tension-compression regime (compare Fig. 2). The crack growth material data from CT specimens, on the other hand, were obtained under pure tensile conditions. There does not exist any confirmed relationship which allows the extrapolation of tensile crack propagation data to describe the tensile-compression crack propagation behaviour. From the experimental evidence which is currently available it can be concluded that the crack propagation rate is underestimated if only the tensile stress component is taken into account and over estimated when the whole stress range is taken into account. In the present analysis a relation was used which lies in between these two limits:

$$\Delta\sigma = \sqrt{(\sigma_{max} - \sigma_{min})\,\sigma_{max}} \qquad (3)$$

Combining equations (2) and (3) the following relation for ΔK is derived

$$\Delta K = \sqrt{(\sigma_{max} - \sigma_{min})\,\sigma_{max}}\; Y\sqrt{a^* + c} \qquad (4)$$

where the geometric factor Y is 2 for a circumferential crack which is small compared to the specimen diameter [9]. If the crack grows to a depth which can no longer be neglected to the bar radius r a finite width correction must be applied to Y [9]:

$$Y^2 = 1{,}25 \,/\, \left[1-(a/r)^{1{,}47}\right]^{2{,}4} \qquad (5)$$

Since most of the life is spent in the range of small crack depths the effect of the finite width correction on the result of the predicted crack propagation life is rather small. Therefore, because of easier treatment, the life calculations were done with a constant Y = 2.

For the description of the crack propagation rate da/dN the relation

$$da/dN = C\,\Delta K^M \qquad (6)$$

was used where C and M are material constants derived from CT specimen measurements (Fig. 10). The crack propagation life N_R between the initial and final crack depth, a_i and a_f resp., was obtained by integration:

$$N_R = \int_{a_i}^{a_f} (da/dN)^{-1}\, da \qquad (7)$$

4. RESULTS

4.1 Specimen results

Fig. 2 shows the stress range in relation to the strain range for LCF tests at 600°C. The measured points closely follow the elastic straight line indicating that the plastic strain component of the hysteresis loop is negligibly small. The maximum stress of the hysteresis loop, on the other hand, is considerably influenced by plastic relaxation (compare the curve maximum stress vs. maximum strain).

Fig. 4 shows the strain range - life curve at 600°C for smooth and grooved specimens. The groove depth of each specimen is indicated in the figure. The figure shows that a groove depth of about 50 microns leads to a reduction of about one order of magnitude in life or a factor of about 1,5 in strain range.

After testing the fracture surface was evaluated with respect to the mean striation density by SEM. The striation density was determined in relation to the crack depth. Starting point for measuring the crack depth was the specimen's surface, i.e. the crack depth includes the groove depth. In most cases the fatigue crack growth rate was about the same at all points around the groove leading to a concentric circular crack front growing to the specimen's axis. In the cases where the groove depth was not evenly distributed the highest crack propagation rates were related to the site of maximum groove depth.

Fig. 5 shows the results of the striation density evaluation for two strain range levels (0,005 and 0,007) at 600°C and Fig. 6 for 0,007 at 400°C. The figures include the predicted striation density according to equation (6). Though the scatter of the striation density values is large the correlation between prediction and experiment is satisfactory.

The integration of the CT sepcimen results according to equation (7) gives the crack propagation life as a function of the initial crack depth for 0,005 and 0,007 strain range at 600°C and 0,007 strain range at 400°C (Fig. 7,8 and 9, resp.). As final crack length a fixed value of 2mm was taken for all specimens since N_R is not very sensitive to the choice of a_f. The actual scatter of the a_f values was between 2 and 3mm.

The influence of the strain ratio on the striation density is demonstrated in Fig. 11. The influence of a tensile mean stress (R = o) significantly reduces the striation density compared with zero mean stress (R = -1). The large scatter of the striation density values makes it impossible to verify or disprove the correctness of equation (3) to describe the influence of mean stress.

The shapes of the fatigue cracks so far considered were such that the crack grows nearly concentrically, i.e. parallel to the specimen's surface. In Fig. 12 the striation density is plotted for a fatigue crack starting at a single point (gauge length mark). The crack propagates with a shape which is close to a semicircle. Since the geometric factor Y in equation (4) for a semicircular crack is smaller than for a straight one (1,27 and 2,0 resp.) the predicted as well as the experimentally verified striation density is significantly higher.

4.2 Case study groove in the bore of a turbine engine disc

The following case study is intended to show that the results of grooved specimen tests can be successfully used to predict the behaviour of machining marks at critical areas of rotating engine components. The engine component which was investigated was a turbine disc of the powder metallurgical nickel-base alloy U700 PM. In order to determine the cyclic life of the disc bore the disc was submitted to a cyclic spin test at 600°C. During one cycle of this test the spinning speed of the disc is accelerated from zero to a fixed maximum and subsequently decelerated again to zero. The test was continued until interuption by bursting occured after 3100 cycles. Analysis showed that the failure was due to a fatigue crack (henceforth called crack (1)) starting from a groove of about 35 microns depth in the bore (Fig. 13). The critical crack depth for final failure of this crack was about 4mm. In the bore of the same disc a second fatigue crack was found (crack (2)) which also has its origin at a groove. The groove depth of crack (2) is only 8 microns and the final depth of the fatigue crack about 200 microns, i.e. well below the critical depth of 4mm. Besides these two cracks no other cracks were found in the bore. This suggests that the fatigue life of the disc was substantially influenced by these grooves. This is supported by the fact that material data from smooth round bar specimen tests give a fatigue life of about 10000 cycles at 600°C at comparable strain conditions as in the disc bore during the cyclic spin test. However, when the test was performed with specimens with a circumferential groove of about 40 microns depth similar to the groove related to crack (1) in the disc the specimen fatigue life decreased to about 3000 cycles consistent with the disk life.

Good agreement was also found with respect to the striation density in relation to the crack depth for the two disc cracks and a grooved specimen (Fig. 14). Fig. 15 shows the residual crack propagation life to failure (i.e. 4mm crack depth) obtained by integration of the data in Fig. 14 as a function of the crack depth. The fatigue life of the disc is very close to the crack propagation life curve. This means that the effect of the groove in the bore is very similar to a fatigue crack of the same size and shape.

It is an interesting question whether the fatigue life of the disk could be improved by use of an alternative material. Fig. 16 compares the fatigue life of four nickel-base disc materials of different yield strengths in the range of 850 to 1120 MPa. Smooth round bar specimens indicate a strong increase in fatigue life with increasing strength. With a groove of 40 microns in depth the advantage of the high strength material disappears and the fatigue life even tends to decrease (probably due to the higher mean stress). The reason for this is that with increasing strength only the crack initiation life is raised while the crack propagation behaviour is rather unaffected (Fig. 17).

5. DISCUSSION AND CONCLUSIONS

5.1 Small grooves in the range between 20 to 100 microns on smooth specimens strongly influence fatigue life of nickelbase alloys (Fig. 4)

5.2 At high strain ranges the residual life is close to the crack propagation life predicted by fracture mechanics assuming that a groove behaves like a crack (Fig. 8 and 9)

5.3 At a lower strain range the specimen fatigue life is much longer than predicted by fracture mechanics (Fig. 7). The probable reason is that the crack initiation period and the life spent in the near threshold crack propagation regime can no longer be neglected.

5.4 According to literature data of nickel-base superalloys [6] the threshold value of ΔK for crack growth is about 10 MN $m^{-3/2}$. The crack depth derived from equation (4) for ΔK = 10 MN $m^{-3/2}$ is included in Fig. 7, 8 and 9. Groove depths below these values result in a fatigue life which is close to the life of smooth specimens (i.e. zero groove depth in Fig. 7, 8 and 9).

5.5 In the range of crack depths larger than about 100 microns the crack propagation rate was monitored by fractographic evaluation of the striation density. The correlation between striation density and predicted crack growth behaviour was found to be rather good for different strain ranges, temperatures and crack shapes. This indicates that the growth of even physically very small cracks can be reasonably well described by conventional fracture mechanics.

5.6 The comparison of nickel-base disk materials of different strengths showed large differences in the fatigue life of smooth specimens but only slight variations for specimens with a groove of 40 microns (Fig. 17).

5.7 The LCF life of a turbine disc containing a groove in the bore was fairly well predicted by tests with grooved specimens. This shows that this approach is suitable to assess the defect tolerance of critical sites of engine components.

5.8 It is often found that shot peening is of limited use or even detrimental in smooth areas and at high applied stresses [10]. However, it is an open question whether the LCF life can be improved when small surface defects are present. The most important beneficial effects of shot peening on fatigue life are due to the

- production of a compressive stress on the surface
- smoothing of the surface leading to a reduction of the defect size and stress concentration factor.

The present results show no significant improvement in the fatigue life due to shot peening (Fig. 7, 8 and 9). Since the number of specimens was very small no statistical evaluation is possible which allows the determination of a small improvement within a factor of 2. Yet it can be concluded that the large decrease in the fatigue life due to small grooves cannot be compensated by shot peening.

Because of the high temperature and strain range the compressive stresses in the surface layer were probably quickly reduced. Furthermore, Fig. 11 shows that the possible gain in crack propagation life by decreasing the mean tensile stress is rather limited.

The strongest effect of shot peening is to be expected in the range where crack initiation makes an important contribution to the fatigue life, since it is well known that the crack initiation life can be much improved by decreasing the mean stress. The gain in life by decreasing the groove depth is much higher in this range than for pure crack propagation. The shot peening applied to the specimens of this investigation resulted in a decrease of the groove depth of about 10 to 20 microns. The gain in life according to Fig. 7, 8 and 9 is beyond the accuracy of the measurements of this investigation.

5.9 The results clearly demonstrate the substantial decrease in defect tolerance with increasing stress range due to

- a reduction of the minimal defect size which is able to propagate
- an increased crack propagation rate
- a decrease of the critical crack depth for final failure (not treated in this paper)
- a decreased capability to compensate the effects of defects by shot peening.

6. LIST OF SYMBOLS

a	crack depth including groove depth
a^*	crack depth
a_i	initial crack depth
a_f	final crack depth
c	notch depth
C	material constants of equation (6)
ΔK	stress intensity range
K_t	stress concentration factor
M	material constants of equation (6)
N_R	crack propagation life
R	strain ratio
r	radius of round bar specimen
$\Delta\sigma_{root}$	stress range in the notch root
$\Delta\sigma$	nominal stress remote from a notch
σ_{max}	maximum stress of the hysteresis loop
σ_{min}	minimum stress of the hysteresis loop
Y	geometric factor

7. REFERENCES

1. Cowles, B.A., SIMS, D.L., WARREN, J.R., Miner, R.V.: Cyclic behaviour of turbine disk alloys at 650°C. Journal of engineering materials and technology, 102 (1980) 356-363

2. Jablonski, D.A.: The effect of ceramic inclusions on the low cycle fatigue life of low carbon astroloy subjected to hot isostatic pressing, Materials science and engineering, 48 (1981) 189-198

3. Betz, W., Track, W.: Structural defects govering the potential use and limitations of powder metallurgy nickel base materials, 109th AIM annual meeting, Las Vegas, (1980)

4. Law, C.C., Blackburn, M.J.: Effects of ceramic inclusions on fatigue properties of a powder metallurgical nickel-base superalloy, Proceedings of the 1980 international powder metallurgy conference, Washington D.C.

5. König, G., Track, W., Betz, W.: Assessment of the LCF behaviour of a PM nickel-base alloy for turbine disk application, Metal powder report, 38 (1983) 19-25

6. Van Stone, R.H., Krueger, D.D. and Duvelius L.T.: Use of a d-c potential drop crack monitoring method in the development of defect tolerant disk alloys in fracture mechanics, ASTM STP 91, American Society for Testing of Materials (1983), II 553-578

7. Huff, H., König, G.: Damage tolerance of aero-engine disks in proceeding of the twelfth international committee on aeronautical fatigue held at Toulouse, France, May 1983, Centre d'Essais Aeronautique de Toulouse

8. Dowling, N.E.: Fatigue at notches and the local strain and fracture mechanics approaches in fracture mechanics, ASTM STP 677, American Society for Testing and Materials, (1979) 247-273

9. Gray, T.G.F.: A closed form approach to the assessment of practical crack propagation problems in fracture mechanics in engineering practice, Stanley (Editor), Applied Science Publishers (1977), 123-147

10. Hertzberg, R.W.: Deformation and fracture mechanics of engineering materials, John Wiley & Sons (1976) 438

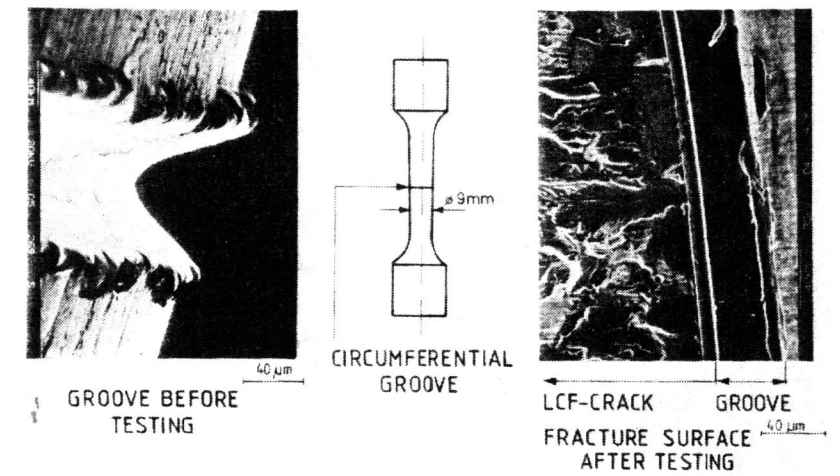

a)

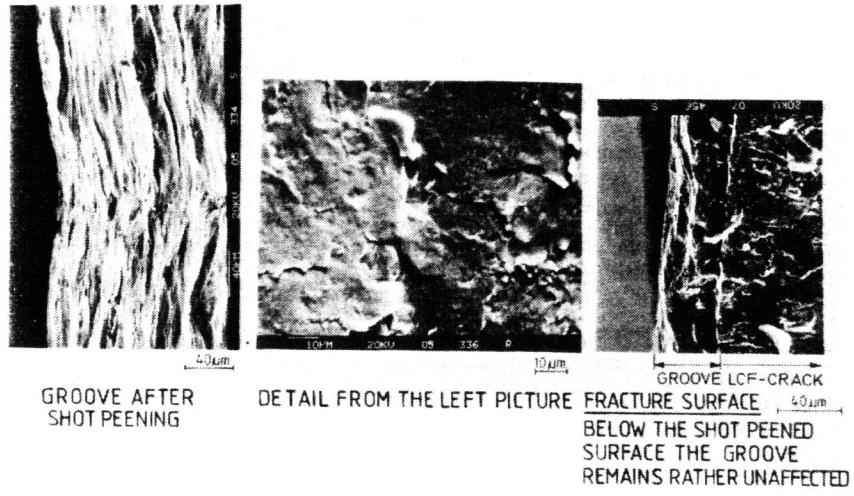

b)

Fig. 1: Circumferential groove in round bar specimen

a) unpeened
b) after shot peening

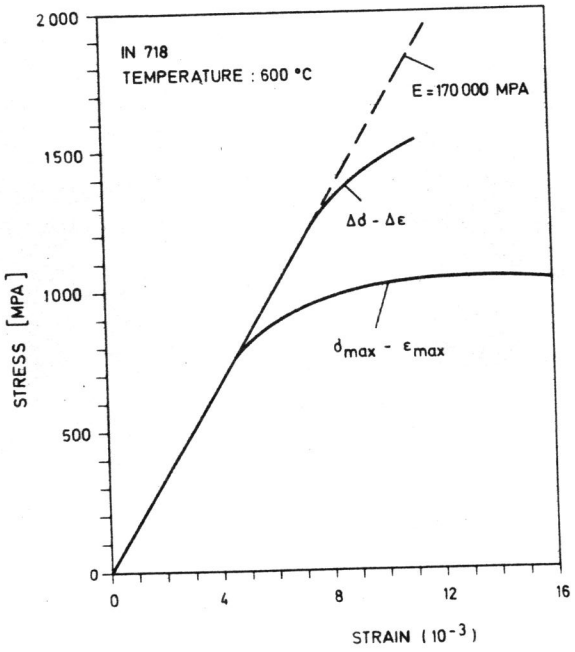

Fig. 2: Cyclic stress-strain curve including stress range vs. strain range and maximum stress vs. maximum strain.

MICROSTRUCTURE OF IN 718

ANNEALED 980°C, AIR COOLED AT ROOM TEMPERATURE
AGED 8H AT 720°C, FURNACE COOLED 620°C AND HELD
AT 620°C FOR A TOTAL AGING TIME OF 18H.
AIR COOLED AT ROOM TEMPERATURE

Fig. 3: Representative micrograph of the microstructure of IN 718.

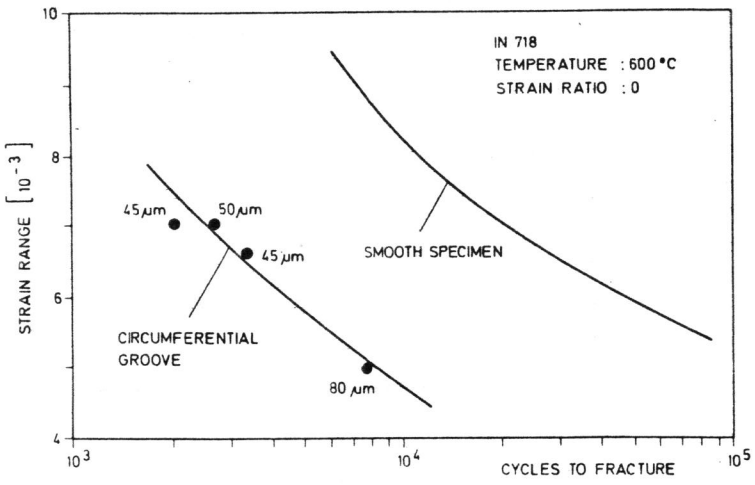

Fig. 4: Strain range - life diagramme for specimens with and without grooves. The numbers indicate the groove depth in microns.

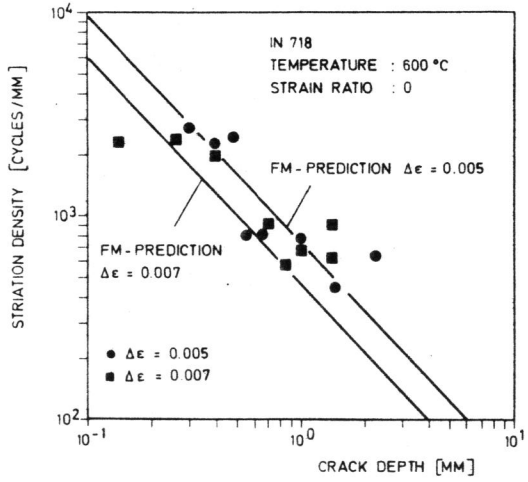

Fig. 5: Infuence of strain range on striation density as a function of crack depth at 600 °C. Comparison with prediction.

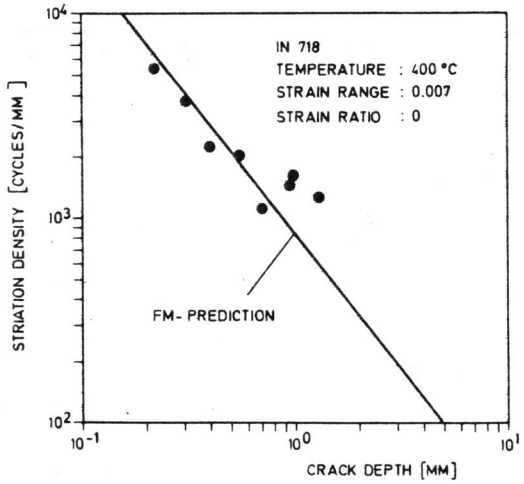

Fig. 6: Comparison between striation density as a function of crack depth and fracture mechanics prediction at 400 °C.

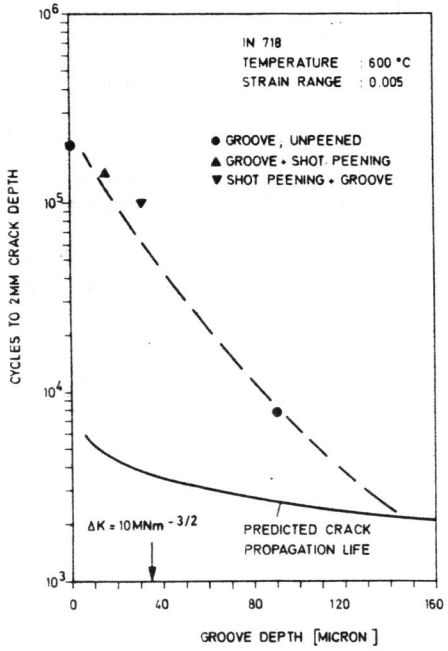

Fig. 7: Fatigue life in relation to the groove depth. Comparison with predicted crack propagation life.

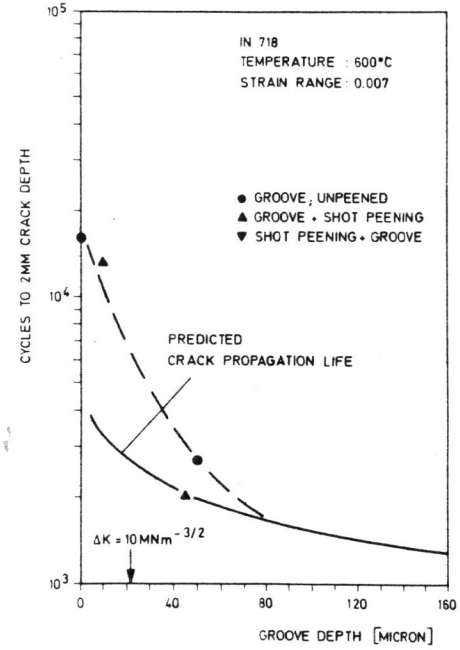

Fig. 8: Fatigue life in relation to the groove depth. Comparison with predicted crack propagation life.

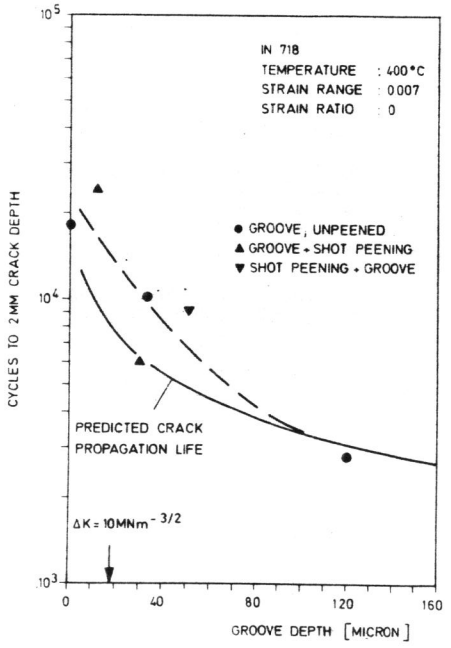

Fig. 9: Fatigue life in relation to the groove depth. Comparison with predicted crack propagation life.

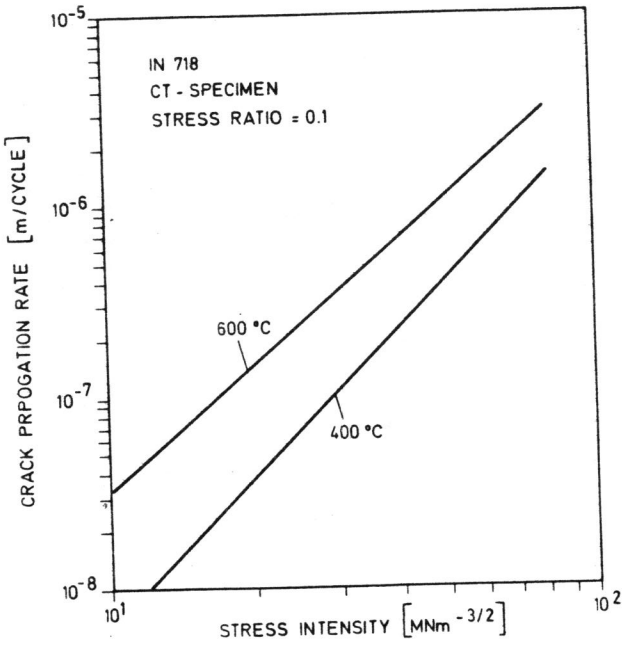

Fig. 10: Crack propagation rate as a function of stress intensity range.

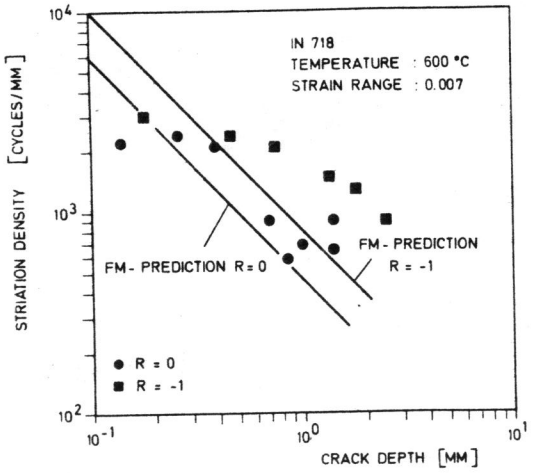

Fig. 11: Influence of the strain ratio on the striation density. Comparison with prediction.

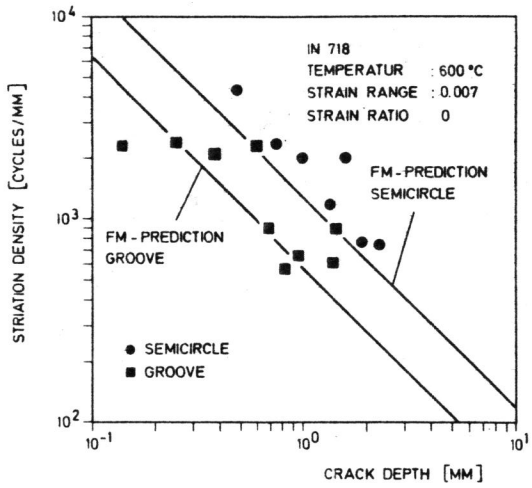

Fig. 12: Influence of the crack shape on the striation density. Comparison with prediction.

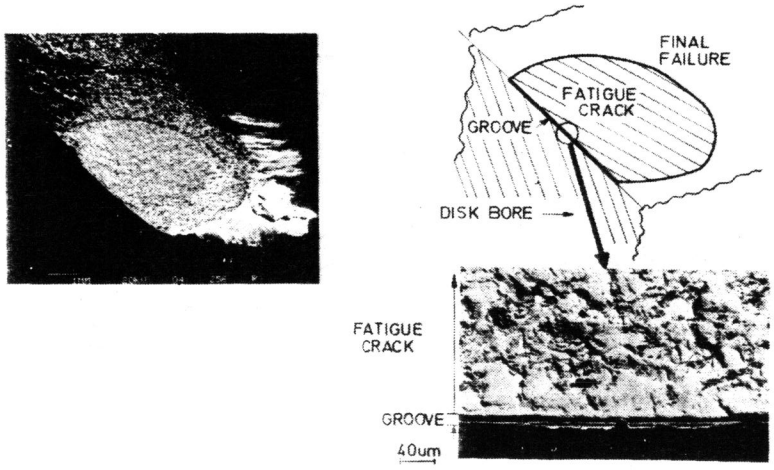

Fig. 13: Crack (1) in disk bore

a) survey
b) groove at the crack initiation site

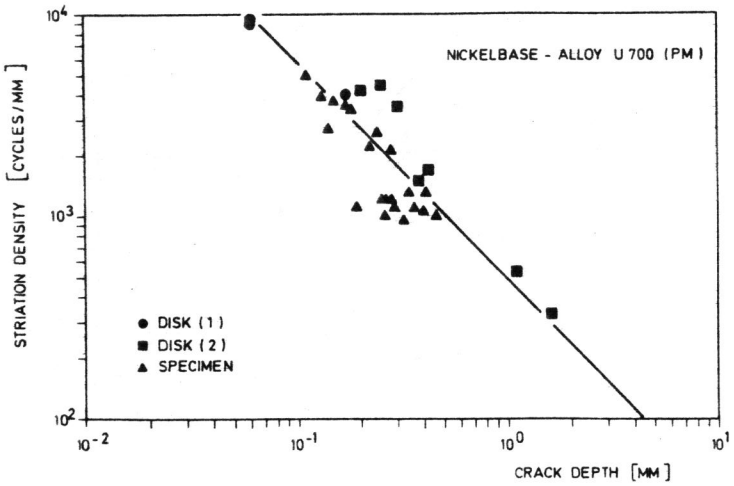

Fig. 14: Comparison between the striation density of crack (1) and (2) in the disk bore and in a round bar specimen.

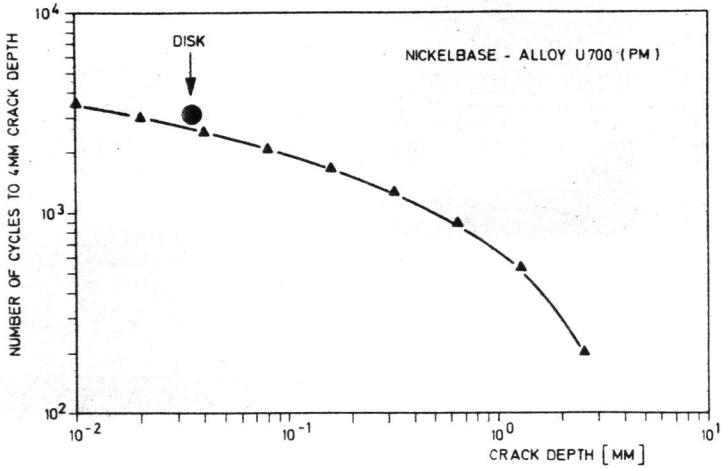

Fig. 15: Comparison between disk life and crack propagation life.

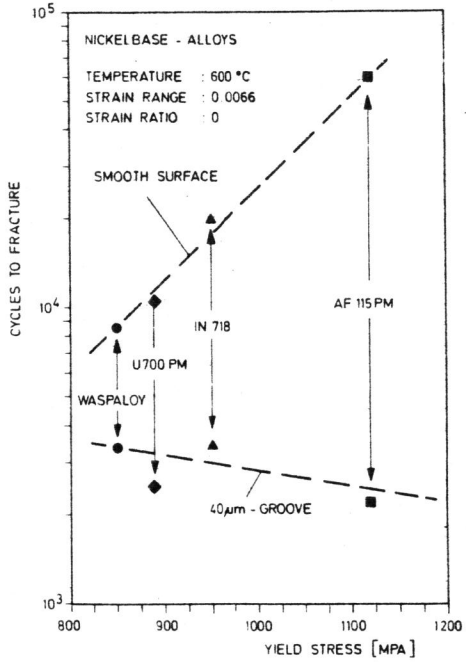

Fig. 16: Comparison of the fatigue life of specimen with (groove depth: 40 microns) and without groove between nickelbase alloys of different yield strengths.

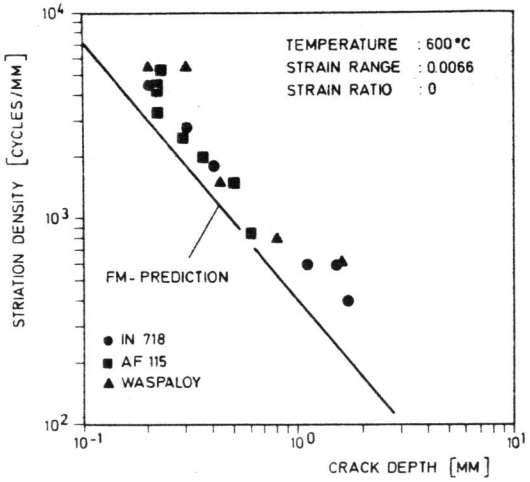

Fig. 17: Comparison between the striation density of different nickelbase alloys.